Marine Biology (2020) 167:66
https://doi.org/10.1007/s00227-020-03680-3

ORIGINAL PAPER

The cell-surface protein composition of a coral symbiont, *Breviolum psygmophilum*, reveals a mechanism for host specificity and displays dynamic regulation during temperature stress

Contessa A. Ricci[1] · Abu Hena Kamal[2] · Jayanta Kishor Chakrabarty[2] · Bren E. Ledbetter[1] · Saiful M. Chowdhury[2] · Laura D. Mydlarz[1]

Received: 16 July 2019 / Accepted: 17 March 2020 / Published online: 19 April 2020

Abstract
The symbiosis between corals and dinoflagellates in the family Symbiodiniaceae is threatened by warming trends that induce coral bleaching, or symbiosis breakdown. Current models of symbiosis breakdown involve an immune response to an elevation in reactive oxygen species that ultimately results in the loss of the symbiont. However, the intimate nature of the symbiosis implies an important role for the symbiont surface as a point of interaction between partners. The response of symbiont cell surface proteins to experimental temperature stress was, therefore, investigated using a cell surface biotin probe. Cell-surface protein composition was found to be dynamically regulated in response to heat stress, particularly after 24 h of exposure to heat treatment. This pattern was primarily driven by an increased abundance in heat shock proteins, demonstrating that stress experienced by the symbiont can manifest at the cell surface. Elements known to activate host immunity were also increased in response to temperature stress, further demonstrating an avenue by which the symbiont can elicit a host immune response independent of reactive oxygen species. This work documents the cell surface protein composition of a Symbiodiniaceae species for the first time and highlights host–symbiont interaction mechanisms that may be important during symbiosis breakdown.

Introduction

Coral reefs are important tropical ecosystems that are both economically (Spalding et al. 2017) and culturally (Cvitanovic et al. 2013) valuable. Their persistence in nutrient-poor tropical waters (Hoegh-Guldberg 1999) is made possible by an intracellular symbiosis formed between the coral animal and dinoflagellates in the family Symbiodiniaceae (formerly genus *Symbiodinium*) (LaJeunesse et al. 2018). These symbionts transfer metabolites (Sogin et al. 2017) and photosynthetic products (Hoegh-Guldberg et al. 2007) that supplement a coral's energy requirements for vital life processes such as growth (Little et al. 2004), calcification (Colombo-Pallotta et al. 2010), and reproduction (Edmunds and Spencer Davies 1986). Warming trends over the past several decades have threatened this symbiosis in many ways. The most well-known threat is coral bleaching, which results from the loss of the symbiont itself (Weis 2008) or from bleaching of the symbiont's photopigments (Hoegh-Guldberg 1999). It is understood as a breakdown in symbiosis (Baker 2003), particularly when bleaching results from the loss of the symbiont cell.

Bleaching is suspected to result through processes such as: exocytosis of the symbiont cell, apoptosis or necrosis of the host cell containing the symbiont, pinching off the portion of the host cell occupied by the symbiont, or detachment of the entire host cell (Gates et al. 1992). Coral bleaching is generally believed to be triggered by oxidative stress that can be either host- or symbiont-derived (Oakley and Davy 2018). However, the role of symbiont cell surface proteins

Responsible Editor: C. Voolstra.

Reviewed by undisclosed experts.

Electronic supplementary material The online version of this article (https://doi.org/10.1007/s00227-020-03680-3) contains supplementary material, which is available to authorized users.

✉ Laura D. Mydlarz
mydlarz@uta.edu

[1] Department of Biology, The University of Texas, 501 S Nedderman Dr Rm 337, Arlington, TX 76019, USA

[2] Department of Chemistry and Biochemistry, The University of Texas, 700 Planetarium Pl, Arlington, TX 76019, USA

and how they change in response to stimuli is worth consideration, as this is a putative site of signal and nutrient exchange and may, therefore, represent an important point of interaction between partners.

Cell surface studies are gaining in importance and it is becoming clear that the extracellular surface of all organisms is actively maintained. In plants, for example, the cell wall is constantly remodeled to accommodate osmotic pressure (Deniaud-Bouët et al. 2017). Additionally, new and emerging roles for processes like extracellular redox in maintaining the intracellular redox state (Jones et al. 2015) are coming to light. In the coral-Symbiodiniaceae symbiosis, cell surface elements such as lectins and glycans have been historically viewed as crucial for successful symbiont infection of host tissues (Logan et al. 2010; Davy et al. 2012; Jimbo et al. 2010; Koike et al. 2004), although recent evidence suggests that these may be more important for post-phagocytic processes (Parkinson et al. 2018). Regardless, despite the importance of this subcellular locale, the symbiont cell-surface protein composition remains unknown. Furthermore, it is also unknown if this composition is dynamic in nature, and if so, what role that may play during thermally induced symbiosis breakdown.

To investigate this, the present study sought to determine the effect of elevated temperature on protein composition at the symbiont cell surface in vitro. Proteins were isolated from the symbiont cell surface using a membrane-impermeable biotin probe (Li et al. 2013; Pelz et al. 2018) on intact symbiont cells with three hypotheses in mind: (1) that the cell-surface protein abundance will change under elevated temperature; (2) that the symbiont cell surface will exhibit stress-mitigating mechanisms under elevated temperature; and (3) that changes occurring at the symbiont cell surface have the potential to elicit immune responses from a host. We found evidence to support all three of these hypotheses and document the first cell surface protein composition of a Symbiodiniaceae species. This work highlights host–symbiont interaction mechanisms that may be important during symbiosis breakdown.

Methods

Study design

Breviolum psygmophilum (formerly *Symbiodinium psygmophilum*, clade B (LaJeunesse et al. 2018); isolated from *Oculina diffusa,* Western Atlantic, Bermuda) was obtained from T. LaJeunesse (Pennsylvania State University) and grown in the Mydlarz lab. Three replicate cultures for the control treatment and three replicate cultures for the heat treatment were grown up to a target density of 500,000 cells/ml. Cultures were grown at 26 °C under a 12-h light/dark cycle at an irradiance of approximately 55 µmol quanta m^{-2} s^{-1} (measured with an LI-COR model LI-250 light meter, LI-COR Environmental) in ASP-8A medium (Chang et al. 1983; McGinty et al. 2012). Light conditions remained the same throughout the experiment. Once cultures reached target density, each replicate culture was separated into three 5 ml subsample volumes (referred to as replicate subsamples henceforth) that were collected and processed at 0-h, 12-h, and 24-h time points after exposure to treatment. 0-h subsamples were collected and processed immediately and were not exposed to either treatment condition.

Replicate subsamples were placed in individual water baths (e.g., 12-h and 24-h replicate subsamples for replicate 1 were in an individual water bath, while 12-h and 24-h replicate subsamples for replicate 2 were placed in a separate water bath) (supplementary figure S1). Water baths were fitted with heaters set to target temperatures (26 °C ± 1 °C for control treatment and 32 °C ± 1 °C for heat treatment to simulate bleaching-inducing conditions). Air pumps were used to circulate water for an even temperature distribution. All water baths were initially set to control treatment temperatures. Once cultures were placed in their respective water baths, heat treatment water baths were subjected to a 2-h temperature ramp. Control treatment water baths remained at a constant temperature during this time. Time of exposure began once the temperature ramp was completed.

Experimental sample processing

At time of collection, replicate subsamples were removed from treatment and pelleted in a benchtop centrifuge at 959×*g* for 10 min. At this speed, it was microscopically confirmed that Symbiodiniaceae cells do not lyse. Intact cells were washed thoroughly using sterile 1× PBS at room temperature. All washes and incubations were conducted using 1× PBS when specified. Although 1× PBS may induce hypoosmotic stress, differences in protein expression and abundance should still result from temperature treatments as each sample was handled identically. Additionally, the exposure time during washing and incubation was relatively minimal.

Replicate subsamples were then incubated for 30 min at room temperature with a membrane-impermeable, cleavable biotin probe (Sulfo-NHS-SS-Biotin, G-Biosciences) (supplementary figure S2). This probe is used commonly in cell-surface studies (e.g., Elschenbroich et al. 2010; Li et al. 2013; Pelz et al. 2018) due to its hydrophobic nature. In this system, the biotin probe is conjugated to a sulfonated NHS ester by a cleavable disulfide linker (Elschenbroich et al. 2010). The sulfo-group transfers hydrophobicity to the probe, and the cleavable property negates the need to chemically unbind the biotin motif from avidin when rescuing isolated proteins (Elschenbroich et al. 2010). This was ideal for

a cell-surface study in Symbiodiniaceae, because cell walls are negatively charged (Shomer et al. 2003) and, as such, the negatively charged biotin probe used would not be able to cross it. The probe will, therefore, primarily detect proteins on the external face of the symbiont cell wall.

To quench the biotinylation reaction after incubation with the biotin probe, 25 mM tris buffer (Trizol, Sigma-Aldrich) was added. After 5 min at room temperature, time point subsamples were spun down in a benchtop centrifuge at 15,330 × g for 5 min, washed thoroughly with sterile PBS, and resuspended in sterile PBS after the final wash (Howes et al. 2010; Jo et al. 2010; Suzuki et al. 2010). *Breviolum psygmophilum* cells were then lysed via bead beating with glass beads for 1 min.

Isolation of biotin-labeled cell surface proteins was conducted by avidin affinity purification using spin columns and monomeric avidin (G-Biosciences). Following established protocols (Lee et al. 2009; Shimus et al. 1985), replicate subsamples were incubated in spin columns with avidin for 30 min at room temperature. Avidin-bound proteins were freed using 50 mM DTT to cleave the probe's disulfide bond via reduction. Freed proteins were rescued via spinning out into a collection tube. The resulting protein isolates were considered cell-surface protein enriched.

Protein isolates were then precipitated using a modified chloroform and methanol protocol (Ferro et al. 2000), wherein the reagents were added to the protein samples in a 3:4:1 v/v/v ratio (protein/methanol/chloroform) and centrifuged in a benchtop centrifuge at 15,330 × g at 4 °C. DTT was removed by resuspending the precipitated protein pellet in 10% SDS and undergoing a second round of precipitation. Once DTT was removed, pellets were resuspended in 1% SDS and protein quantification of replicate subsamples was performed using a BCA assay (G-Biosciences) in a microplate spectrophotometer (BioTek).

Nanospray-LC–MS/MS

4 ng of protein per replicate subsample were tryptically digested in solution following established protocols (Chakrabarty et al. 2016). In summary, protein isolates were incubated with 10 mM DTT at 56 °C for 45 min under continuous agitation. Protein isolates were then incubated with 10 mM iodoacetamide in the dark at room temperature for 30 min. 50 mM ammonium bicarbonate was then added followed by trypsin in a 1:50 w/w ratio (trypsin/protein) and incubated overnight at 37 °C under continuous agitation. After tryptic digestion, 0.1% formic acid was added to neutralize the pH and protein isolates were then dehydrated in a speedvac (Vacufuge plus, Eppendorf). Once dehydrated, protein isolates were reconstituted in 0.1% formic and introduced to a Velos Pro Dual-Pressure Linear Ion Trap Mass Spectrometer (ThermoFisher Scientifc). Nanospray-LC–MS/MS was carried out using a data-dependent protocol. Protein fragmentation was achieved by collision-induced dissociation (CID).

Isolated protein sequences were identified from mass spectra using Proteome Discoverer software (ver. 2.0, ThermoFisher Scientifc). Using the Sequest HT algorithm within the software, spectra were matched against a translated *Breviolum psygmophilum* transcriptome publicly available from Reef Genomics databases (Liew et al. 2016; Parkinson et al. 2016). Sequest HT criteria were as follows: the proteolytic enzyme was indicated as trypsin; two missed cleavages were allowed; precursor mass range of 350–5000 Da; fragment mass tolerance of ± 2.5 and 0.6 Da; peptide charges excluded + 1 (Kamal et al. 2018).

Data set building

A decoy search strategy was employed in Proteome Discoverer software using a 5% False Discovery Rate (FDR) (Wilhelm et al. 2014). *Breviolum psygmophilum* proteins in replicate subsamples were considered identified with high confidence at ≤ 5% FDR if they met either of the following criteria: (a) ≥ 2 peptides were detected in ≥ 2 replicates; or (b) ≥ 1 peptide was detected in all three replicates (Kamal et al. 2018). Using these criteria, a data set of 147 proteins was compiled (supplementary table S1). Proteome Discoverer utilizes the label-free method of spectral counting to quantify protein expression (peptide spectral matches; i.e., PSMs). PSMs of confidently identified proteins were normalized as % total PSMs per replicate subsample (Kamal et al. 2018).

To annotate the 147 proteins identified within the *B. psygmophilum* transcriptome, their sequences were BLASTed against the Uniprot KB Swiss-Prot database. An *e* value ≥ e^{-5} was considered a confident annotation (Mayfield et al. 2018). If a *B. psygmophilum* sequence could not meet the criteria for confident annotation, it was BLASTed against the entire Uniprot KB database (i.e., Swiss-Prot and TrEMBL databases).

Once annotated, GO terms (Gene Ontology) and literature searches were utilized to categorize the proteins into functional groups based on their roles when expressed at the cell surface or secreted into the extracellular space. In instances where GO terms agreed with the known extracellular role, the GO term was used to group proteins of the same function. In all other instances, proteins were grouped according to known functions documented in the literature (supplementary table S2). Literature searches were conducted by providing the search term "extracellular", "secreted", or "cell surface" before the protein name, and only manuscripts found with these searches were used to determine if proteins possessed a cell surface or extracellular presence. Additionally, if these searches yielded proteins known to interact with

a host immune system when present at the cell surface or in the extracellular space, then it was classified as either immune-activating, -regulating, or -suppressing (e.g., cell surface heat shock protein 70 promotes phagocytosis and is, therefore, classified under immune activation). The regulatory category encompassed proteins with known regulatory roles or whose extracellular effects on a host immune system were conflicting.

These methods found that 67 of the 147 proteins identified have a documented extracellular function in the literature and 12 proteins have an extracellular presence but an unknown function. Statistical analyses were carried out on these proteins (79 in total) to determine how treatment and length of treatment affected the composition of proteins and protein function at the cell surface. 47 proteins were known chloroplast constituents and were, therefore, considered contamination. Chloroplast contamination is not uncommon in cell wall/cell surface studies in dinoflagellates (Li et al. 2012; Wang et al. 2004a). Chloroplast contamination is likely due to the extreme peripheral position of the large dinoflagellate chloroplasts (Lee et al. 2014). Chloroplast constituents did not change with heat (supplementary figure S3) and were not considered further.

Validation of NodG homolog and Nod homolog searches among Symbiodiniaceae

A nod factor G (nodG) homolog was identified (comp8899_c0_seq1.p1) in *Breviolum psygmophilum* and classified under signal transduction (Table 1). Because of its putative roles in symbiosis, a special attention was paid to the validation of its presence within the *B. psygmophilum* transcriptome. The presence of nod factors in other Symbiodiniaceae was also investigated for this reason. A Pfam protein domain search was compared between the *B. psygmophilum* nodG and the reviewed uniprot nodG sequence which it was matched to via BLAST (nodG, uniprot ID P72332 from from *Rhizobium sp.* strain N33). Additionally, an EMBL-EBI pairwise sequence alignment using the EMBOSS Water algorithm was conducted with the following criteria: EBLOSUM62 was used at the matrix, gap penalty was set to 10, and extend penalty was set to 0.5 (Madeira et al. 2019).

Investigations into nod factor presence in other Symbiodiniaceae were carried out on six species whose genomes or transcriptomes are publicly available on Reef Genomics databases: *Breviolum aenigmaticum*, *B. minutum*, *B. pseudominutum*, *B. psygmophilum*, *Cladocopium* (species unknown), and *Fugacium kawagutii*. Symbiodiniaceae sequences were BLASTed against a databased composed of the 148 nod factor sequences available through the Uniprot KB database. An *e* value $\geq e^{-5}$ cut-off was imposed. The top ten strongest BLAST hits plus the sequence of the nodG homolog identified in this study were then phylogenetically compared using the Clustal Omega algorithm and bacterial nodI as an outgroup (unprot ID Q39GT7, *Burkholderia lata*) (Madeira et al. 2019).

Finally, the same six Symbiodiniaceae species were queried for the presence of nod factors A, B, C, and D (NodABCD). NodABCD is necessary for the synthesis of the lipochitooligosaccharide backbone of all nod factors (Roche et al. 1996), which are later modified by other nod factors for host specificity (Wang et al. 2018). Symbiodiniaceae genomes/transcriptomes were BLASTed against a database comprised of all available NodABCD sequences available through the Uniprot KB database. An *e* value $\geq e^{-5}$ cut-off was again imposed.

Statistical analysis

All statistical analyses were conducted using R statistical software (R Development Core Team 2015). Identified proteins were divided into groups based on protein function (i.e., functional groups). Bray–Curtis distances were utilized by similarity percentages analysis (i.e., SIMPER analysis) to calculate the strongest drivers of differences observed between control and heat-treated samples (Clarke 1993; Warton et al. 2012). From SIMPER analyses, the most influential functional groups and/or individual proteins within a functional group were determined. SIMPER was carried out using the 'simper' function in the R package 'vegan' (Oksanen et al. 2018). PCA was conducted on the cumulative protein abundance for functional groups of interest using the 'ggbiplot' function in the R package 'ggbiplot' (Vu 2011).

To address the possible correlation in protein expression within resampled experimental units, repeated measures MANOVA was conducted using the 'RM' function in the R package 'MANOVA.RM' (Friedrich et al. 2018). Non-parametric *t* tests were then conducted on the cumulative protein abundance for influential functional groups (e.g., cumulative abundance of proteins with immune modulatory functions in control vs. heat-treated samples). Within functional groups, non-parametric *t* tests were also carried out on the abundance of individual proteins that were determined to be influential by SIMPER (e.g., abundance of the protein V-type H^+-ATPase in control vs. heat-treated samples).

To quantify the biological significance of the differences observed in protein abundance observed, effect size was calculated using Cohen's *d* estimation (Cohen 1992a, b; Rice and Harris 2005). Effect size is defined as the discrepancy between the null hypothesis and the alternate hypothesis (Cohen 1992a). The small sample size ($n=3$ per treatment) in combination with the variability observed between replicates can potentially underinflate statistical significance at $\alpha=0.05$. This can, therefore, obscure findings of biological importance. Effect size is thus reported in addition to *p* values

Table 1 Protein functional groups

Functional group	*B. psygmophilum* transcriptome sequence	Protein name
Adhesion	comp36757_c0_seq1.p1	Elongation factor 1-alpha
	comp11356_c0_seq1.p1	Enolase
	comp18414_c0_seq5.p1	Enolase
	comp29485_c0_seq1.p1	Enolase
	comp29838_c0_seq2.p1	Enolase
	comp33094_c0_seq4.p1	Glutamine synthetase
	comp36464_c0_seq1.p1	Glutamine synthetase
	comp37011_c1_seq2.p1	Glutamine synthetase
	comp37015_c0_seq2.p1	Glyceraldehyde-3-phosphate dehydrogenase
	comp37083_c0_seq2.p1	Glyceraldehyde-3-phosphate dehydrogenase
	comp34391_c0_seq1.p1	Phosphoglycerate kinase
	comp33801_c0_seq4.p1	Triosephosphate isomerase
	comp37351_c0_seq1.p2	Triosephosphate isomerase
	comp37849_c0_seq1.p1	Triosephosphate isomerase
Cell structure	comp1748_c0_seq1.p2	Actin
	comp35046_c0_seq3.p2	Actin
	comp33420_c0_seq2.p1	Collagen alpha-1(XVII) chain
	comp37901_c0_seq1.p1	Collagen alpha-1(XVII) chain
	comp61911_c0_seq1.p1	Major outer membrane lipoprotein
	comp24819_c0_seq1.p1	Tubulin
	comp36850_c0_seq5.p1	Tubulin
	comp37027_c0_seq2.p1	Tubulin
	comp37107_c0_seq1.p1	Tubulin
CO_2 uptake	comp35964_c0_seq3.p1	Carbonic anhydrase
	comp36098_c0_seq3.p1	Carbonic anhydrase
Extracellular ATP	comp36516_c0_seq2.p1	ATP synthase gamma chain
	comp36952_c0_seq2.p1	ATP synthase gamma chain
	comp38541_c0_seq1.p1	ATP synthase subunit alpha
	comp25655_c0_seq1.p1	ATP synthase subunit beta
	comp27837_c0_seq1.p1	ATP synthase subunit beta
	comp34697_c0_seq1.p1	ATP synthase subunit beta
	comp37979_c0_seq1.p1	ATP synthase subunit beta
Extracellular redox	comp33468_c0_seq1.p1	Acyl-CoA dehydrogenase
	comp35869_c0_seq6.p2	Cytochrome c-550
	comp35093_c0_seq2.p2	Cytochrome c6
	comp39261_c0_seq1.p1	Dihydrolipoyl dehydrogenase
	comp18413_c0_seq1.p1	Fumarate reductase
	comp22274_c0_seq2.p1	Fumarate reductase
	comp36145_c0_seq1.p1	Fumarate reductase
	comp36488_c0_seq5.p1	Fumarate reductase
	comp36454_c0_seq1.p1	Glutathione S-transferase
	comp33055_c0_seq2.p1	L-lactate dehydrogenase
	comp37134_c0_seq1.p1	Pyruvate dehydrogenase
Signal transduction	comp11845_c0_seq1.p1	14-3-3-like protein
	comp36800_c0_seq1.p1	14-3-3-like protein
	comp35699_c0_seq1.p1	Calreticulin
	comp35990_c0_seq1.p1	Cell division cycle protein 48 homolog
	comp29762_c0_seq1.p1	Developmentally-regulated G-protein 2
	comp14901_c0_seq1.p1	Nicotinamide phosphoribosyltransferase
	comp8899_c0_seq1.p1	Nodulation protein G

Table 1 (continued)

Functional group	*B. psygmophilum* transcriptome sequence	Protein name
	comp36444_c0_seq1.p2	Serine/threonine-protein phosphatase
	comp33615_c1_seq2.p1	Ubiquitin
Ion homeostasis	comp37477_c0_seq1.p1	V-type proton ATPase catalytic subunit A
	comp18453_c0_seq2.p1	Putative K (+)-stimulated pyrophosphate-energized sodium pump
Protein folding	comp8280_c0_seq1.p1	Chaperonin CPN60
	comp23514_c0_seq4.p1	Heat shock 70 protein
	comp33298_c0_seq4.p1	Heat shock 70 protein
	comp36948_c0_seq1.p1	Heat shock 70 protein
	comp36974_c0_seq1.p1	Heat shock 70 protein
	comp7486_c0_seq1.p1	Heat shock 70 protein
	comp24965_c0_seq1.p1	Heat shock 90 protein
	comp36621_c0_seq5.p1	Heat shock 90 protein
	comp36855_c0_seq1.p1	Heat shock 90 protein
	comp37297_c0_seq1.p1	Heat shock 90 protein
	comp16455_c0_seq1.p2	Peptidyl-prolyl *cis–trans* isomerase
	comp36920_c0_seq4.p1	Peptidyl-prolyl *cis–trans* isomerase
	comp38944_c0_seq1.p1	Peptidyl-prolyl *cis–trans* isomerase
	comp18648_c0_seq1.p1	Protein disulfide-isomerase
Unknown	comp8484_c0_seq1.p2	3-ketoacyl-CoA thiolase
	comp31713_c0_seq1.p1	3-ketoacyl-CoA thiolase
	comp22970_c0_seq1.p1	ATP-citrate synthase
	comp30984_c0_seq1.p1	ATP-citrate synthase
	comp35289_c0_seq2.p1	Elongation factor 2
	comp34171_c0_seq1.p1	Isocitrate lyase
	comp30131_c0_seq1.p1	Phosphoenolpyruvate carboxykinase
	comp38011_c0_seq1.p1	Phosphoenolpyruvate carboxykinase
	comp18185_c0_seq1.p1	Phosphoenolpyruvate carboxylase
	comp31985_c0_seq1.p2	S-adenosylmethionine synthase
	comp37675_c0_seq1.p1	Succinate dehydrogenase flavoprotein subunit
	comp38376_c0_seq1.p1	Succinate-CoA ligase subunit beta

List of proteins isolated from the *Breviolum Psigmophilum* cell surface, categorized into functional groups based on roles at the cell surface. Proteins categorized via GO terms (Gene Ontology databases) and literature searches

to provide more transparent and accurate statistical interpretation (Greenland et al. 2016; Wasserstein and Lazar 2016). Cohen's *d* was calculated using the 'cohen. *d*' function in the R package 'EffSize' (Torchiano 2018). A small-effect size is a Cohen's $d \sim 0.2$, a medium-effect size is a Cohen's $d \sim 0.5$, and a large-effect size is a Cohen's $d \sim 0.8$ (values noticeably lower than 0.2 are considered negligible, while values noticeably greater than 0.8 are considered very large-effect sizes) (Rice and Harris 2005; Torchiano 2018).

Results

Constitutive cell-surface protein composition of *Breviolum psygmophilum*

Control samples and heat samples at 0 h of exposure to treatments are pooled and considered the constitutive state of the *Breviolum psygmophilum* cell surface. A total of

147 proteins were identified at ≤5% FDR (supplementary table S1). 79 identified proteins are known to be either secreted or actively released into the extracellular space, or expressed at the cell surface in various prokaryotic and eukaryotic species (supplementary table S2). These 79 proteins were used in statistical analyses for this study. 12 proteins had either no literature documentation of cell surface presence or the literature concerning the protein was conflicting. These proteins were also considered contamination. Three proteins could not be identified by BLAST.

The 79 proteins known to occur at the cell surface or in the extracellular space encompassed nine functional groups: protein folding, cell structure, adhesion, CO_2 uptake, extracellular ATP synthase, extracellular redox, signal transduction, ion homeostasis, and an unknown category representing proteins whose function is unknown when expressed in the extracellular space (they will not be addressed further as a result; Table 1). Adhesion proteins represent the most abundant functional group at the cell surface of *B. psygmophilum*, while proteins representing the ion homeostasis functional group were least abundant (Fig. 1).

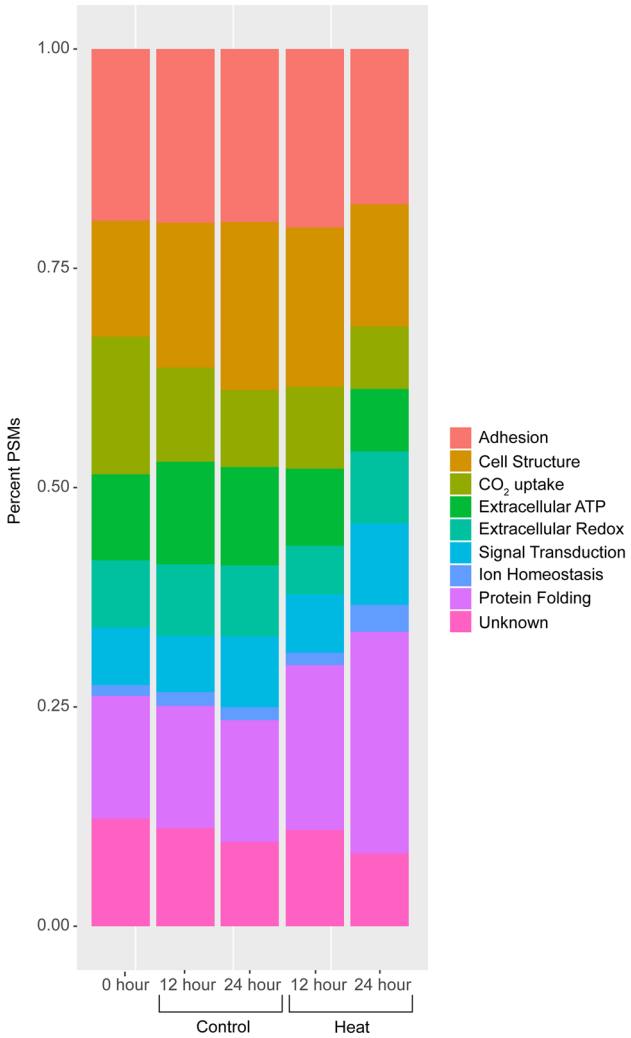

Fig. 1 Stacked plot depicting relative abundance of functional groups. Percentages reported are based on the average abundance of each functional group between treatment replicates. Adhesion: $n=14$ proteins; cell structure: $n=9$; CO_2 uptake: $n=2$; extracellular ATP: $n=7$; extracellular redox: $n=11$; signal transduction: 9; ion homeostasis: $n=2$; protein folding: $n=14$; unknown = 12. *Y*-axis represents percent normalized peptide spectral matches (PSMs)

Nodulation factors present in *Breviolum psygmophilum* and other *Symbiodiniaceae* species

The *B. psygmophilum* nodG homolog identified is, indeed, a putative nodulation factor. Pairwise sequence alignment between *B. psygmophilum* nodG homolog and *Rhizobium* sp. strain N33 nodG (uniprot ID P72332) achieved a high sequence alignment: 48.4% identity match, 66.5% similarity, and 3.6% gaps (Fig. 2a). The overall alignment score was 547. Pfam searches between the *Breviolum psygmophilum* nodG homolog and the *Rhizobium sp.* strain N33 nodG also displayed identical protein domain structure (Fig. 2b).

Potential nodulation factors are ubiquitous in Symbiodiniaceae, with a total of 6,557 matches identified across the six Symbiodiniaceae species investigated (supplementary file 1). Potential NodABCD homologs were found in all species investigated as well (supplementary file 2). All six species were represented in the top ten strongest hits found via BLAST. The Nod sequences investigated grouped according to Symbiodiniaceae species (Fig. 2c).

Response of *Breviolum psygmophilum* cell-surface proteins to heat

Proteins at the cell surface were responsive to temperature stress, particularly when time is taken into account (Table 2). One protein was identified as uniquely present in the control samples (comp36516_c0_seq1.p1; ATP synthase subunit) and one protein was identified as uniquely present in the heat-treated samples (comp35699_c0_seq1.p1; calreticulin). For the shared proteins (i.e., proteins found in both control and heat-treated samples), total protein abundance does not differ between treatments until after 24 h of exposure to heat treatment ($p=0.400$, Cohen's $d=-0.440$, Fig. 3). Differences are primarily seen in the abundance between the proteins uniquely expressed in either the control or heat-treated samples: after 24 h of exposure to heat treatment, abundance of the heat-treatment-unique protein was greater than that of the control treatment ($p=0.176$, Cohen's $d=-0.894$, Fig. 3). The control-treatment-unique protein was not present after 24 h.

Total abundance of proteins within functional groups showed differences through time and by treatment (Fig. 4). The functional groups driving the differences observed

Fig. 2 Validation of nodG in Breviolum psygmophilum **a** sequence alignment between *B. psygmophilum* nodG homolog and Rhizobium sp. nodG (uniprot ID P72332); **b** Pfam protein domains present in *B. psygmophilum* nodG homolog and *Rhizobium* sp. nodG; **c** Phylogenetic analysis of top ten strongest BLAST hits for nod factors across Symbiodiniaceae species. (*) denotes *B. psygmophilum* nodG identified in the current study

Table 2 Statistical comparison of treatment on all response variables

Whole model RM MANOVA		
Effect		*p* value
Treatment		0.7
Time		0.189
Treatment * time		0.132
Functional group		**< 0.001**
Treatment * functional group		0.398
Time * functional group		**0.002**
Treatment * time * functional group		**0.017**
Post hoc SIMPER analysis		
Functional group	Average	Cumsum
Protein folding	0.054	0.217
Cell structure	0.039	0.372
Adhesion	0.032	0.503
CO_2 uptake	0.032	0.632
Extracellular ATP	0.027	0.739
Unknown	0.023	0.832
Extracellular redox	0.022	0.922
Signal transduction	0.011	0.964
Ion homeostasis	0.009	1

Repeated-measures MANOVA outcome and SIMPER post hoc tests to determine largest drivers of difference between treatments. Bold *P* values represent significant effects ($P \leq 0.05$). SIMPER conducted on protein abundance for sequences found within each functional group. "Average" represents average contribution to overall dissimilarity. "Cumsum" represents cumulative contribution to overall dissimilarity

between control and heat-treated samples were, in order of most influential: protein folding, cell structure, adhesion, CO_2 uptake, and extracellular ATP synthase (Table 2). When the most influential functional groups were used to characterize the protein abundance data, only those samples that belong to the 24-h heat treatment were distinct (Fig. 5). This demonstrates that the exposure to 1X PBS was not long enough to substantially affect protein expression. Only those differences at the 24-h time point were considered in further analyses.

Protein responses in the most influential functional groups to heat

The protein-folding functional group was represented by 14 unique proteins that represented five protein types (Table 1). The top two most influential proteins in the protein-folding group were heat shock protein (HSP) 70 and HSP 90 (Table 3, SIMPER cumsum ~ 80%). After 24 h of exposure to heat treatment, both proteins were in greater abundance when compared to control samples ($p = 0.400$ and Cohen's $d = -1.174$, $p = 0.100$ and Cohen's $d = -2.870$; respectively; Table 3, Fig. 6).

Cell structure was represented by nine unique proteins that represented four protein types (Table 1). Tubulin and a major outer membrane lipoprotein were the two most influential proteins (Table 3, SIMPER cumsum ~ 83%). After 24 h of exposure to heat treatment, tubulin abundance decreased ($p = 0.400$ and Cohen's $d = 0.981$, Table 3, Fig. 6), while the abundance of the major outer membrane

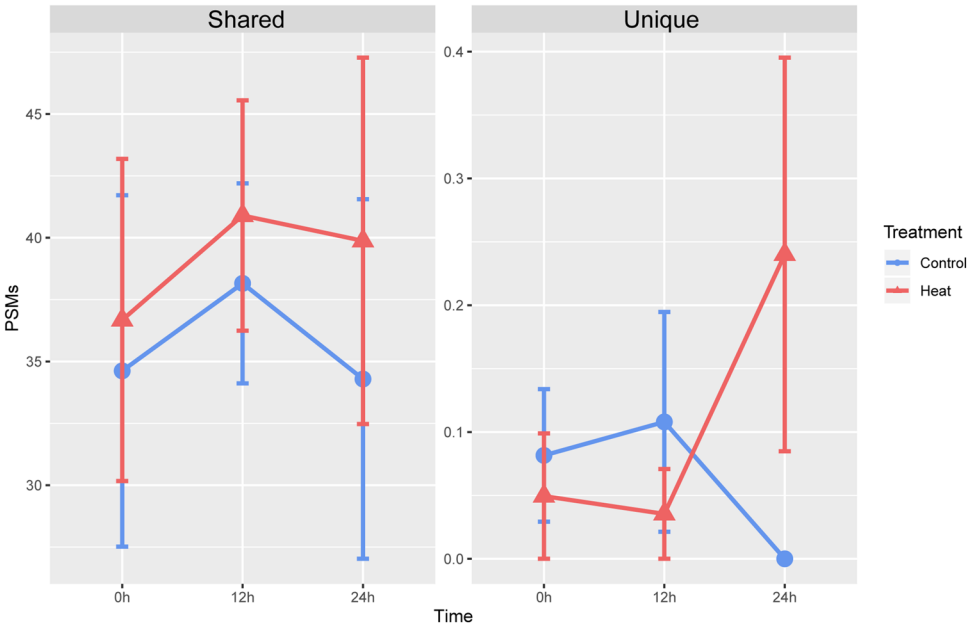

Fig. 3 Total abundance of proteins found in each treatment. Left: total abundance of proteins for sequences found only in either control ($n=1$) or heat-treated ($n=1$) samples. Right: total abundance of proteins for sequences found in both control or heat-treated samples ($n=77$). Blue lines with circles represent control treatment; red lines with triangles represent heat treatment. At 24 h of exposure, shared proteins do not differ in abundance ($p=0.400$, Cohen's $d=-0.440$), but unique proteins do ($p=0.176$, Cohen's $d=-0.894$). *Y*-axis represents normalized peptide spectral matches (PSMs)

lipoprotein increased ($p=0.100$ and Cohen's $d=-1.243$, Table 3, Fig. 6).

Adhesive proteins were represented by 14 unique proteins that encompassed six protein types (Table 1) and were most influenced by enolase and triosephosphate isomerase (TPI) (Table 3, SIMPER cumsum ~ 55%). After 24 h of exposure to heat treatment, neither protein differed in abundance compared to control treatments ($p=0.633$, Cohen's $d=-0.441$ and $p=0.960$, Cohen's $d=0.043$; respectively; Table 3, Fig. 6).

CO_2 uptake was represented by two unique proteins that were both identified as carbonic anhydrase by BLAST (Table 1). Extracellular ATP synthase was similarly represented by four unique proteins that were all identified as ATP synthase subunits by BLAST (Table 1). After 24 h of exposure to heat treatment, carbonic anhydrase did not differ from control samples in abundance ($p=0.931$, Cohen's $d=0.078$, Table 3, Fig. 6); however, variation between samples was much higher for heat-treated samples vs. control samples. ATP synthase decreased in abundance in heat-treated samples compared to control samples ($p=0.378$, Cohen's $d=0.814$, Table 3, Fig. 6).

Responses of extracellular redox, signal transduction, and ion homeostasis proteins to heat

Extracellular redox was represented by 11 unique proteins that represented seven protein types (Table 1). Fumarate reductase and cytochrome c were the most influential proteins within the extracellular redox functional group (Table 3, SIMPER cumsum ~ 64%). Fumarate reductase was found in greater abundance in heat-treated samples compared to control samples, while cytochrome c did not differ in abundance, but was greater in between-sample variation ($p=0.700$, Cohen's $d=-0.954$ and $p=1.000$, Cohen's $d=0.214$; respectively; Table 3, Fig. 6).

The signal transduction group was represented by nine unique proteins that represented eight protein types (Table 1). The 14-3-3-like protein and calreticulin were the most influential proteins within this functional group (Table 3, SIMPER cumsum ~ 40%). 14-3-3 increased in abundance after 24 h of exposure to heat treatment, while calreticulin was only found in heat-treated samples ($p=0.200$, Cohen's $d=-1.459$ and $p=0.197$, Cohen's $d=-1.564$; respectively; Table 3, Fig. 6). Ion homeostasis was represented by a K^+-stimulated sodium pump and a V-type proton ATPase (Table 1). Only the V-type proton ATPase was found in greater abundance after 24 h of exposure to heat treatment ($p=0.391$, Cohen's $d=-0.865$, Table 3, Fig. 6).

Immune modulatory proteins present at the *Breviolum psygmophilum* cell surface and their response to heat

Proteins known to modulate a host immune system via immune activation, suppression, or regulation were identified in cell-surface protein isolates (supplementary table S3). Proteins were assigned to each category based on information available within the literature (supplementary table S3). The regulatory category encompassed proteins with known regulatory roles or whose extracellular effects on the host immune system were conflicting.

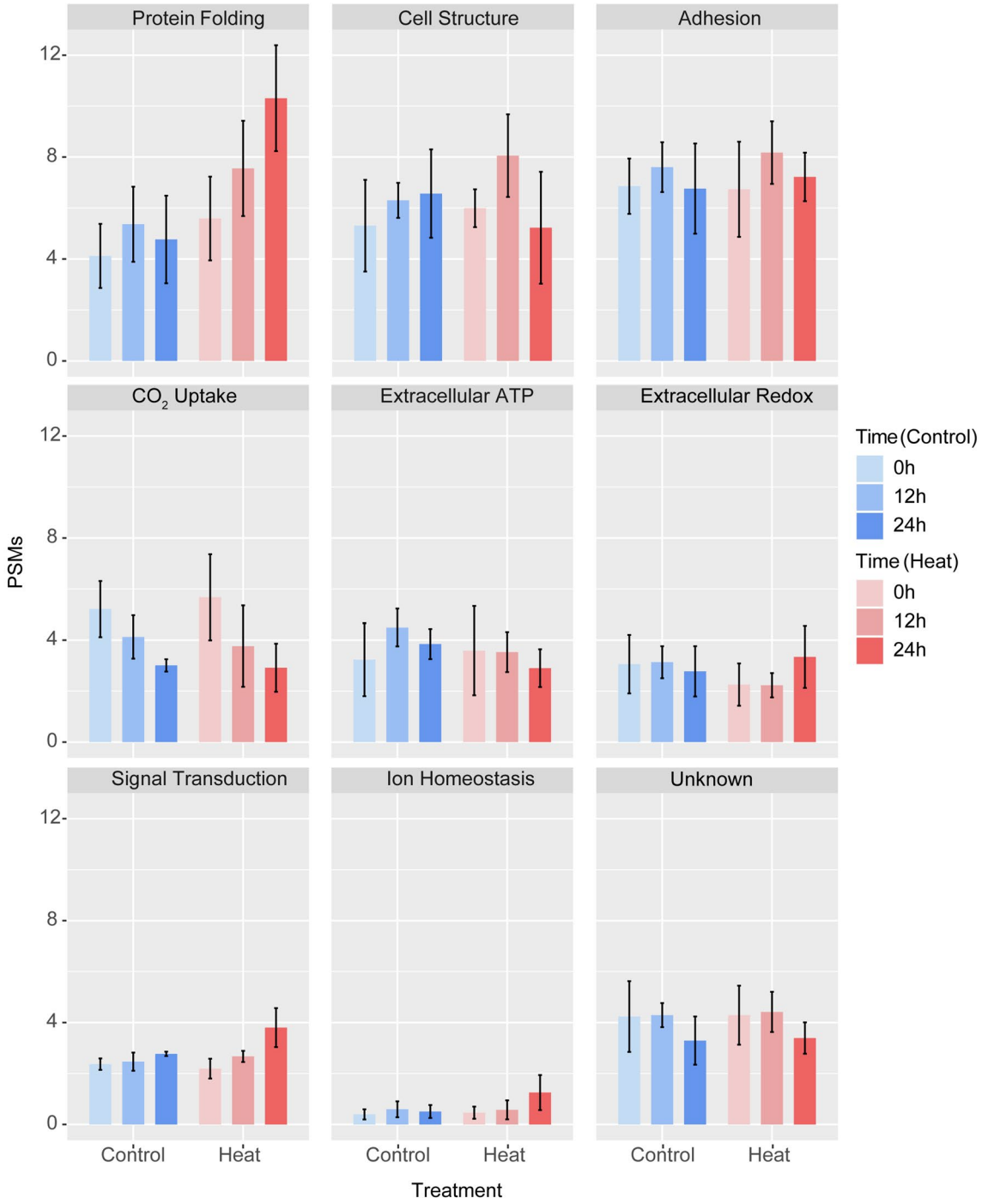

Fig. 4 Total abundance of proteins found in each treatment for each functional group through time. Blue hues represent control treatments; red hues represent heat treatments. Adhesion: $n = 14$ proteins; cell structure: $n = 9$; CO_2 uptake: $n = 2$; extracellular ATP: $n = 7$; extracellular redox: $n = 11$; signal transduction: 9; ion homeostasis: $n = 2$; protein folding: $n = 14$; unknown = 12. *Y*-axis represents normalized peptide spectral matches (PSMs)

Immune modulatory proteins were affected by both treatment and time (RM MANOVA, Table 4). Differences only at the 24-h time point are addressed: cumulative abundance of all immune-activating proteins increased in response to heat ($p = 0.1$, Cohen's $d = -2.131$, Table 4, Fig. 7), while the cumulative abundance of all immune-suppressing proteins decreased ($p = 0.505$, Cohen's $d = 0.816$, Table 4, Fig. 7); immune regulatory proteins were not responsive to heat ($p = 0.4$, Cohen's $d = 0.585$, Table 4, Fig. 7).

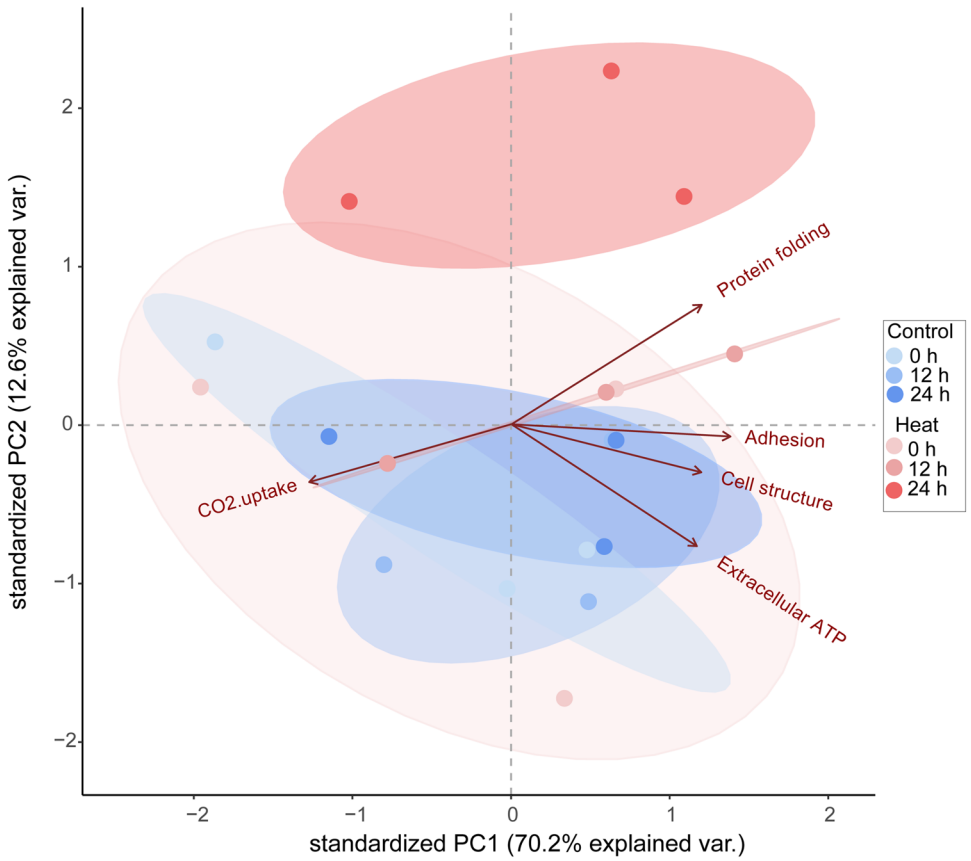

Fig. 5 PCA plot comparing treatments to functional groups

Discussion

The nature of the coral-Symbiodiniaceae symbiosis implies an important role for the symbiont surface as a possible point of interaction between the coral cell and the intracellular symbiont. As such, proteomic investigation at this locale is important in understanding potential mechanisms in partner dynamics. In this study, the *Breviolum psygmophilum* transcriptome developed by Parkinson et al. (2016) was used as a database to inform protein identification from cultured *B. psygmophilum*, and only proteins encoded within the *B. psygmophilum* genome were identified as a result. Our investigation reveals elements of host-specific interaction mechanisms and shows cell-surface proteins are responsive to heat stress. We also show that stress-mitigating mechanisms have the potential to influence a host immune system.

The biotin probe utilized within this study ensures that a cell-surface-enriched protein fraction was analyzed due to the probe's hydrophobic nature (Elschenbroich et al. 2010). Identified proteins were further validated for cell surface presence or absence and classified into functional groups based on rigorous, non-biased literature searches. While we did observe the presence of proteins that are not exclusively extracellular, it is coming to light that many proteins can have multiple subcellular locations (e.g., Jeffery 2015; Gancedo et al. 2016), and that many proteins can be destined for the cell surface and extracellular space despite lacking a proper signal peptide (Robinson et al. 2016). Exosomes and microvesicular bodies (MVBs) are gaining momentum as a mechanism for the transport of intracellular proteins to the cell surface, and may represent a possible explanation for the presence of these proteins in the cell surface-enriched protein fraction of *B. psygmophilum*. Indeed, MVBs are acknowledged as ubiquitous across the tree of life and have been observed traversing the cell walls of plants, fungi, and bacteria (Rodrigues et al. 2015; Samuel et al. 2015). Alternatively, the presence of these proteins may also be explained by cell lysis in culture, and adherence of the proteins to the cell surface of intact cells. However, the thorough washings conducted during sample processing minimize this as a possibility. Furthermore, the lack of canonical intracellular markers that do not have a documented cell surface presence [e.g., CYP450, ER (Scotcher et al. 2017); histone, nuclear (Yang et al. 2004); G6Pase, ER (Scotcher et al. 2017); rab proteins, endosomal (Smith et al. 2016); ras proteins, endosomal (Arike and Peil 2014); RPL11, ribosomal (Brodersen and Nissen 2005); HSP60, mitochondrial (Bonifati et al. 2003)] indicate that intracellular contamination was minimal.

Table 3 Statistical comparison of two most influential proteins within each functional group

Most influential functional groups				
Functional group	Average	Cumsum	*P* value	Effect size
Protein folding				
HSP 70	0.206	0.438	0.400	**−1.174**
HSP 90	0.168	0.795	0.100	**−2.870**
Cell structure				
Tubulin	0.304	0.652	0.400	**0.981**
Major outer membrane lipoprotein	0.083	0.830	0.100	**−1.243**
Adhesion				
Enolase	0.073	0.230	0.700	0.441
Triosephosphate Isomerase	0.069	0.546	1.000	0.043
CO_2 uptake				
Carbonic anhydrase	0.263	1	0.700	0.079
Extracellular ATP				
ATP synthase	0.263	1	0.400	**0.814**
Others				
Extracellular redox				
Fumarate reductase	0.239	0.474	0.700	**−0.954**
Cytochrome C	0.082	0.637	1.000	0.214
Signal transduction				
14-3-3-like protein	0.085	0.200	0.200	**−1.459**
Calreticulin	0.083	0.395	0.197	**−1.564**
Ion homeostasis				
V-type H + ATPase	0.259	0.746	0.507	**−0.865**
Putative K + stimulated pyrophosphate-energized sodium pump	0.088	1	1.000	0.040

Based on SIMPER analysis on proteins contributing to the differences observed within functional group in response to treatment. Effect size was calculated by Cohen's d estimation. Bold *P* values represent significant effect for non-parametric *t* tests ($P \leq 0.05$). Bold effect sizes represent large-effect size values. SIMPER conducted on protein abundance for sequences found within each functional group. "Average" represents average contribution to overall dissimilarity. "Cumsum" represent cumulative contribution to overall dissimilarity. Unknown functional category not reported

Despite the probe's hydrophobic properties, a large number of chloroplast constituents were isolated. Chloroplast contamination is not uncommon in cell wall/cell surface studies in plants and algae (e.g., Li et al. 2012; Wang et al. 2004a; Calderon-Rodrigues et al. 2014). Some authors have explained their presence as a result of mistargeting by the protein's signal peptide (Slabas et al. 2004). Indeed, proteins destined for the mitochondria can be mistargeted to the cytosol (Wrobel et al. 2015), providing precedence for such a phenomenon. Others have hypothesized a role for the underlying biology of free-living dinoflagellates, whereby individual cells are linked together via an attachment pore are broken apart by a mechanical disturbance that leads to chloroplastic leakage (Li et al. 2012). An alternative possibility for their presence in the current study may be related to the extreme peripheral position of the chloroplast in *B. psygmophilum* (Lee et al. 2014), which may result in co-isolation with proteins specifically bound by the cell surface probe. We currently cannot explain definitively why this was observed. Because chloroplast constituents did not change with heat, they were considered as random contamination that does not represent the intracellular state and were not addressed further.

Constitutive cell-surface proteins of *Breviolum psygmophilum* carry out essential functions

The extracellular matrix and cell membrane carry out important functions. They are often viewed as a first line of defense against assaults on cellular integrity (Deniaud-Bouët et al. 2017) and are also responsible for waste exchange and nutrient uptake (Hahn and Mendgen 2001). In addition, they are important for modulating osmotic pressure (Deniaud-Bouët et al. 2017) and sensing cues from the extracellular environment that lead to cell growth or differentiation (Deniaud-Bouët et al. 2017). Recent advances in cell-surface research are highlighting this dynamic nature across the tree of life (Shi et al. 2016; Lemmon et al. 2016). It is now clear

that cells actively maintain the cell surface and the extracellular space directly adjacent to the cell surface to preserve homeostasis.

At the constitutive state, the adhesive functional group had the highest abundance at the *Breviolum psygmophilum* cell surface and was primarily represented by glycolytic proteins. When expressed at the cell surface, many of these proteins bind to laminin (Amblee and Jeffery 2015), a major constituent of animal extracellular matrices, including those of Cnidaria (Sarras and Deutzmann 2001), and plasminogen (Gancedo et al. 2016), the inactive form of the serine protease plasmin (Aisina and Mukhametova 2014). Of interest is that plasmin is important for the degradation of animal cell extracellular matrices (Chana-Muñoz et al. 2019), and plasminogen-binding proteins have been utilized by a number of pathogens to promote host invasion (Ayon-Nunez et al. 2018). It is, however, unclear if invertebrates possess plasmins (Chana-Muñoz et al. 2019; Chao et al. 2012). The presence of proteins in *B. psygmophilum* that can potentially bind plasminogen may, therefore, simply be relevant for adhesion alone rather than host infection.

The abundance of the adhesive functional group was followed closely by the cell structure and CO_2 uptake proteins. CO_2 uptake was represented by two proteins identified as carbonic anhydrase (CA). In the unicellular green alga *Dunaliella tertiolecta*, cell-surface CA assists in the uptake of CO_2 from the surrounding water (Aizawa and Miyachi 1984). The same role is carried out by cell-surface CA in various other phytoplankton (Mustaffa et al. 2017), including Symbiodiniaceae (Yellowlees et al. 1993; Karim et al. 2011). Cell-surface CA is responsible for dehydrating HCO_{3-} to CO_2, which is then diffused into the cell (Aizawa & Miyachi 1984), although it appears to be the case that symbionts *in hospite* do not readily utilize HCO_{3-} (Yellowlees et al. 1993), and may instead rely on the cnidarian host to concentrate extracellular HCO_{3-} to provide a sufficient level of CO_2 for photosynthesis (Allemand et al. 1998; Furla et al. 2000). This suggests that cell-surface CA may be more relevant in the free-living state. In either case, the identification of cell-surface CA at the cell surface of *B. psygmophilum* corroborates a growing body of literature demonstrating the ubiquity of proteins with pleiotropic (Orjalo et al. 2009; Ebnet 2017) and moonlighting (Jeffery 2015; Gancedo et al. 2016) properties. This is with particular regard to extracellular protein function (Wang and Jeffery 2016).

Other emerging roles for the cell surface are extracellular ATP synthesis (Federica and Antonio 2018) and extracellular redox processes (Banerjee 2012). Extracellular ATP synthase (i.e., eATP synthase) has only recently been accepted as a truly functional complex when expressed at the cell surface (Federica and Antonio 2018) and, as such, is poorly understood. They do, however, have ion regulating properties that are believed to result from the movement of hydrogen ions into and out of the cell during the synthesis and hydrolysis of ATP (Federica and Antonio 2018). There may be as of yet unknown functions at the cell surface of *B. psygmophilum* that rely on eATP synthase or eATP. Extracellular redox, on the other hand, is known to be important in maintaining the intracellular redox environment (Banerjee 2012). Interestingly, extracellular redox modulation has roles in inflammatory processes (Carta et al. 2009) and may, therefore, be an important aspect governing symbiosis dynamics between corals and *B. psygmophilum*.

Nod factors are ubiquitous across Symbiodiniaceae species

Nod factors are secreted lipochitooligosaccharide molecules that are primarily characterized in the plant endosymbiotic bacteria, *Rhizobium*. In the plant-rhizobia model, flavonoids are secreted by the host plant to attract bacteria (Hassan and Mathesius 2012), and the detection of these flavonoids by the bacteria in turn produces Nod factors that are then secreted by the bacteria (Oldroyd and Downie 2004). A complete Nod factor is synthesized by the "common" Nod factors (Nods A,B,C,D), which are responsible for synthesizing the chitin backbone of the molecule (Roche et al. 1996), and the "specific" Nod factors (all other nod factors), which modify the chitin backbone for host specificity (Wang et al. 2018). Upon secretion, Nod factors are perceived by plant LysM proteins, which consist of an extracellular LysM motif and an intracellular protein kinase domain with autophosphorylation properties (Madsen et al. 2011), and perception of a compatible bacteria–Nod factor combination by the plant tissues then causes the iconic root hair deformation and nodulation characteristic of a successful symbiosis (Oldroyd and Downie 2004). Importantly, incompatible Nod factors will prevent a symbiosis from forming (Oldroyd and Downie 2004).

The presence of the nodG homolog in *Breviolum psygmophilum* corroborates the previous reports of Nod factors present in Symbiodiniaceae (e.g., Lin et al. 2015; Weston et al. 2012). The nodG homolog identified at the *B. psygmophilum* cell surface shows high homology to the reviewed *Rhizobium* sp. nodG. The occurrence of other Nod factors across Symbiodiniaceae was thus further explored, as well as the presence of the common Nod factors due to their necessity for the synthesis of the Nod factor backbone. Each of the six Symbiodiniaceae species investigated possessed sequences homologous to Nods A, B, C, and D within their respective genomes/transcriptomes, and the subset of sequences that were phylogenetically investigated show Nod factors grouping by species.

Lectin and glycan interactions between Symbiodiniaceae and the coral host have historically been the favored model for partner specificity (Logan et al. 2010; Wood-Charlson

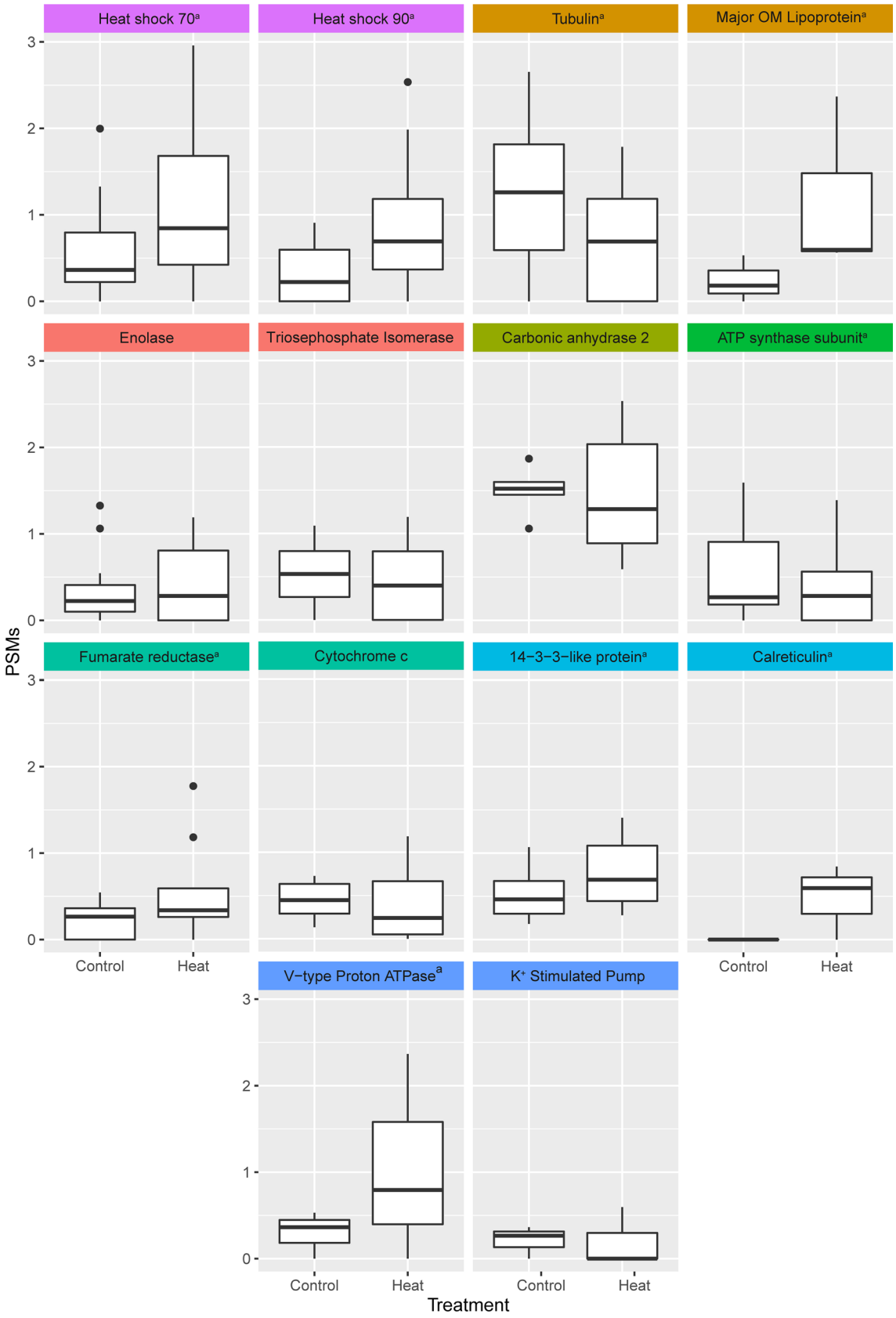
Heat shock 70[a]
Heat shock 90[a]
Tubulin[a]
Major OM Lipoprotein[a]
Enolase
Triosephosphate Isomerase
Carbonic anhydrase 2
ATP synthase subunit[a]
Fumarate reductase[a]
Cytochrome c
14−3−3−like protein[a]
Calreticulin[a]
V−type Proton ATPase[a]
K+ Stimulated Pump
PSMs
0
1
2
3
Control
Heat
Treatment

◂**Fig. 6** Top two most influential proteins for each functional group according to simper. Purple: protein folding; orange: cell structure; red: Adhesion; olive green: CO_2 uptake; green: extracellular ATP; teal: extracellular redox; light blue: signal transduction; blue: ion homeostasis. (*) represents those differences between treatment that are stastically significant; (a) represents those differences with large-effect sizes. Effect size was calculated using Cohen's *d* estimation. *Y*-axis represents normalized peptide spectral matches (PSMs)

et al. 2006). However, recent evidence suggests that other aspects may take part in this process, as manipulation of Symbiodiniaceae glycans does not appear to alter host infection rates (Parkinson et al. 2018). While at present, it is unknown if Nod factors in Symbiodiniaceae carry out the same functions as in *Rhizobium*, nor if the coral host has the machinery necessary to detect and/or respond to them, the presence of Nod factor-like proteins at the *B. psygmophilum* cell surface opens new lines of inquiry when considering alternative elements for partner selection.

The cell-surface of *Breviolum psygmophilum* is responsive to heat stress over time

Heat affects the *Breviolum psygmophilum* cell surface primarily after 24 h of exposure to heat treatment. As such, comparisons were made at the 24-h time point. Protein folding was the most influential functional group driving the differences between control and heat-treated samples. This resulted from an increase in heat shock protein (HSP) 70 and HSP 90 at the *B. psygmophilum* cell surface. HSPs are commonly upregulated in response to stress (Wiersma et al. 2015) and function to protect the existing proteins from denaturing (Hasanuzzaman et al. 2013; Wang et al. 2004b). Here, we show that cell-surface HSPs are a key response to heat stress in *B. psygmophilum*. HSP action may be facilitated by eATP synthase, as both HSP 70 and HSP 90 require ATP to bind target proteins and carry out chaperone functions (Hasanuzzaman et al. 2013; Wang et al. 2004b). It may be of biological importance that eATP synthase decreases in response to heat, while HSP proteins increase. Uncoupling of the two may reflect dysfunction brought on by heat stress. Regardless, the observation of increased HSPs demonstrates that stress experienced by *B. psygmophilum* under elevated temperatures manifests at the cell surface and has implications for an intracellular symbiosis *in hospite*.

Tubulin also decreased after 24 h of exposure to heat. Dynamic tubulin modulation is important for cell wall remodeling (Chan et al. 2010; Ochs et al. 2014), and decreases observed in response to heat are somewhat paradoxical within the context of HSP increases. This is likely because remodeling to accommodate responses such as protein translocation and insertion took place prior to 24 h. Cell wall remodeling in *B. psygmophilum* may, therefore, occur during early responses to stress. Conversely, the abundance of a major outer membrane lipoprotein increases in response to heat after 24 h of exposure. In the dinoflagellate cell wall, these proteins are important for protein binding, lipid anchoring, and calcium binding (Wang et al. 2011), and may have similar roles in the *B. psygmophilum* cell wall.

Increases in extracellular redox proteins demonstrate an increased need by *B. psygmophilum* to maintain their intracellular redox environment, and may result from an increased energy demand that can potentially fatigue redox gradients across the mitochondrial membrane (Banerjee 2012). Related is the increase in the V-type H^+-ATPase, a protein responsible for the transport of protons into and out of the cell (Miles et al. 2017). Responses by both the extracellular redox and ion homeostasis functional groups demonstrate the importance of the cell surface in maintaining the intracellular environment. Importantly, H^+-ATPase was thought to only be expressed by Symbiodiniaceae when in a symbiotic state (Bertucci et al. 2010; Miles et al. 2017). However, this was supported by gene expression alone. Using proteogenomic methods, we show that this protein is indeed found in a Symbiodiniaceae species outside of a symbiosis and that it is responsive to heat stress.

Proteins known to stimulate host immune responses are present at the cell surface of *Breviolum psygmophilum* and increase with heat

Proteins known to modulate a host immune system were present at the *Breviolum psygmophilum* cell surface. Within the 15 proteins detected, three categories could be identified based on literature searches: immune activation (i.e., eliciting an immune response from a host upon detection); immune regulation (i.e., roles in immune activation and resolution); and immune suppression (i.e., preventing or hindering a host immune response). The majority of these proteins (11/15) are known to activate a host immune system. Three proteins, ubiquitin (Majetschak 2011), ATP synthase (Chivasa et al. 2009), and peptidyl-prolyl cis–trans isomerase (Ünal and Steinert 2014), have roles in immune regulation. One protein, nicotinamide phosphoribosyl transferase, is known to suppress a host immune system upon extracellular detection (Audrito et al. 2015).

Although the effect of specific proteins on the coral immune system was not itself investigated, it is a worthwhile consideration when addressing cell-surface proteins. For example, cell-surface heat shock protein 70 can promote phagocytosis (Wang et al. 2006), and inflammatory cytokine production through interaction with TLR2 and TLR4 (Asea et al. 2002). Furthermore, the existence and persistence of an intracellular symbiont ultimately involves the immune system as it inherently implies that the host is not clearing a foreign body.

Table 4 Statistical comparison of treatment on immune modulating proteins

Whole model RM MANOVA		
Effect		*p* value
Treatment		0.437
Time		**0.02**
Treatment * time		0.076
Interaction with immune system		**< 0.001**
Treatment * interaction with immune system		**0.009**
Time * interaction with immune system		**0.04**
Treatment * time * interaction with immune system		0.081
Post hoc non-parametric t test		
Immune modulation	*p* value	Effect size
Activation	0.1	**− 2.131**
Regulation	0.4	0.585
Suppression	0.505	**0.816**

Repeated-measures MANOVA outcome and post hoc tests. Effect size was calculated by Cohen's *d* estimation. Bold *P* values represent significant effects ($P \leq 0.05$). Bold effect sizes represent large-effect size values

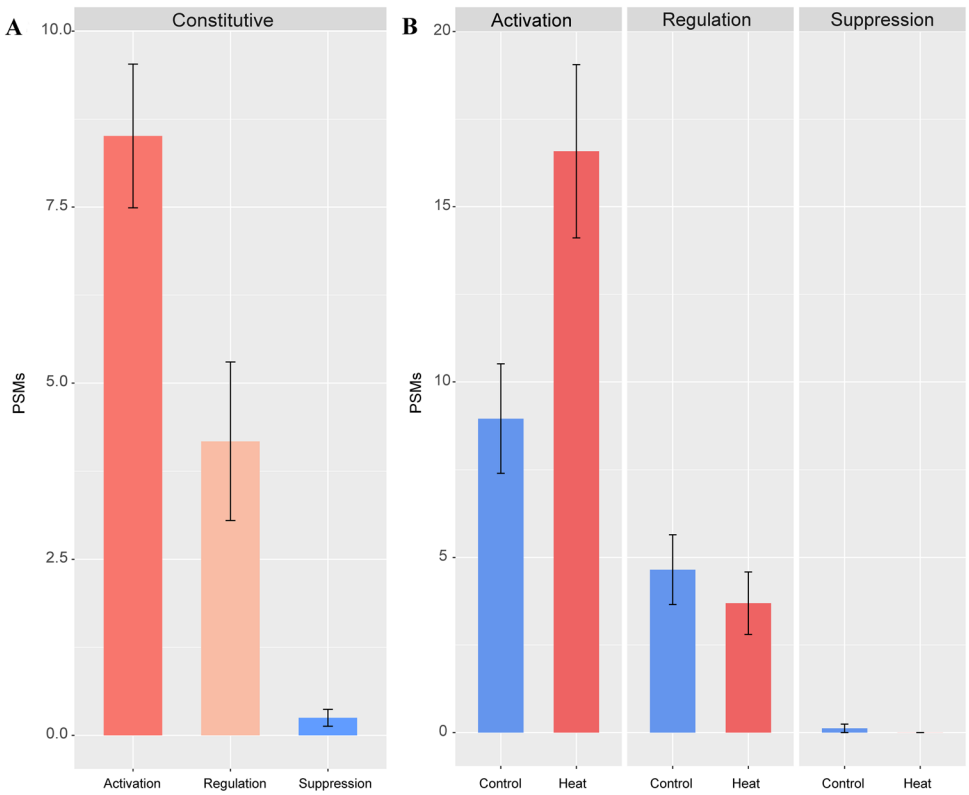

Fig. 7 Response of immune modulation proteins after 24 h exposure to heat. Blue boxes represent control treatments; red boxes represent heat treatments; (*) represents those differences between treatment that are stastically significant; (a) represents those differences with large-effect sizes. Activation: $n = 11$; regulation: $n = 3$; suppression: $n = 1$. Effect size was calculated using Cohen's *d* estimation. *Y*-axis represents normalized peptide spectral matches (PSMs)

In Symbiodiniaceae, persistence within the host is generally attributed to host immune suppression. This is evidenced by phenomena such as corals displaying decreased disease susceptibility when bleached, or in other words, when corals have a lower symbiont load (Merselis et al. 2018) and the upregulation of immune-suppressing TGF-β in the coral host during the onset of symbiosis (Berthelier et al. 2017). It may, therefore, be important that immune-activating proteins increase, while regulating proteins decrease and immune-suppressing proteins virtually disappear after 24 h of exposure to heat stress. Should such a pattern persist when in a symbiotic state, it would support the hypothesis that thermally induced bleaching results from a host immune response against Symbiodiniaceae. It would also support the

hypothesis that the immune response results, in part, from symbiont dysfunction.

Breviolum psygmophilum present an "eat me" signal after experiencing heat stress

Calreticulin was present at the *Breviolum psygmophilum* cell surface after 24 h of exposure to heat stress. Calreticulin typically provides chaperone-like functions in the endoplasmic reticulum (Wang et al. 2004b); however, it is known to accumulate at the cell surface during stress events (Park and Kim 2017). In apoptotic cells, this accumulation can promote cell clearance by serving as an "eat me" signal to phagocytic cells (Park and Kim 2017). Because the symbiosome is established as an arrested phagosome (Mohamed et al. 2016), one possibility is that cell-surface calreticulin "re-activates" the fusion of the symbiosome to the previously inhibited lysosome. Calreticulin could, therefore, serve as a signal for dysfunction to the coral host and induce symbiophagic processes.

Conclusions

The coral-Symbiodiniaceae symbiosis is responsible for the persistence of coral reefs in tropical waters. Rising global temperatures are a primary threat to this symbiosis. This work joins an emerging body of research highlighting the importance of cell-surface modulation. Here, we present the first formal investigation into the response of cell-surface proteins to elevated temperatures in a Symbiodiniaceae species and show that this locale is dynamically modified in response to heat. These data demonstrate that stress experienced within the cell is manifested at the cell surface, and that these proteins have the potential to influence host responses during temperature stress. As coral bleaching (i.e., symbiosis breakdown) continues to decimate reefs, continuing investigation into responsible mechanisms is of vital importance for informing conservation and management practices.

Acknowledgements The authors would like to acknowledge funding from awards IOS-1831860 and OCE-1712134 from the National Science Foundation to LDM. This material is based on work supported by the LSAMP bridge to doctorate fellowship programs under Grant no.1026806 to CAR. We also acknowledge funding from the UT System Proteomics Core Facility Network for a mass spectrometer.

Data availability statement All proteomic data collected and analyzed within the current study are in the Supplementary Tables, or available from the corresponding author upon request. Sequences listed in supplementary material were identified using a translated *Breviolum psygmophilum* transcriptome publicly available from Reef Genomics databases.

Compliance with ethical standards

Conflict of interest The authors declare they have no conflict of interest.

Ethical approval All applicable international, national, and/or institutional guidelines for the care and use of animals were followed.

References

Aisina RB, Mukhametova LI (2014) Structure and function of plasminogen/plasmin system. Russ J Bioorg 40:590–605

Aizawa K, Miyachi S (1984) Carbonic anhydrase located on cell surface increases the affinity for inorganic carbon in photosynthesis of *Dunaliella tertiolecta*. FEBS J 173:41–44

Allemand D, Furla P, Bénazet-Tambutté S (1998) Mechanisms of carbon acquisition for endosymbiont photosynthesis in Anthozoa. Can J Bot 76:925–941

Amblee V, Jeffery CJ (2015) Physical features of intracellular proteins that moonlight on the cell surface. PLoS ONE 10(6):e0130575. https://doi.org/10.1371/journal.pone.0130575

Arike L, Peil L (2014) Spectral counting label-free proteomics. In: Martins-de-Souza D (ed) Shotgun proteomics: methods and protocols. Springer, New York, pp 213–222

Asea A, Rehli M, Kabingu E, Boch JA, Bare O, Auron PE, Stevenson MA, Calderwood SK (2002) Novel signal transduction pathway utilized by extracellular HSP70: role of toll-like receptor (TLR) 2 and TLR4. J Biol Chem 277:15028–15034

Audrito V, Serra S, Brusa D, Mazzola F, Arruga F, Vaisitti T, Coscia M, Maffei R, Rossi D, Wang T, Inghirami G, Rizzi M, Gaidano G, Garcia JG, Wolberger C, Raffaelli N, Deaglio S (2015) Extracellular nicotinamide phosphoribosyltransferase (NAMPT) promotes M2 macrophage polarization in chronic lymphocytic leukemia. Blood 125:111–123

Ayón-Núñez DA, Fragoso G, Bobes RJ, Laclette JP (2018) Plasminogen-binding proteins as an evasion mechanism of the host's innate immunity in infectious diseases. Biosci Rep. https://doi.org/10.1042/BSR20180705

Baker A (2003) Flexibility and specificity in coral-algal symbiosis: diversity, ecology, and biogeography of symbiodinium. Annu Rev Ecol Evol Syst 34:661–689

Banerjee R (2012) Redox outside the box: linking extracellular redox remodeling with intracellular redox metabolism. J Biol Chem 287:4397–4402

Berthelier J, Schnitzler CE, Wood-Charlson EM, Poole AZ, Weis VM, Detournay O (2017) Implication of the host TGFβ pathway in the onset of symbiosis between larvae of the coral *Fungia scutaria* and the dinoflagellate *Symbiodinium* sp. (clade C1f). Coral Reefs 36:1263–1268

Bertucci A, Tambutté E, Tambutté S, Allemand D, Zoccola D (2010) Symbiosis-dependent gene expression in coral–dinoflagellate association: cloning and characterization of a P-type H+-ATPase gene. Proc Biol Sci 277:87–95

Bonifati V, Rizzu P, van Baren MJ, Schaap O, Breedveld GJ, Krieger E, Dekker MC, Squitieri F, Ibanez P, Joosse M, van Dongen JW, Vanacore N, van Swieten JC, Brice A, Meco G, van Duijn CM, Oostra BA, Heutink P (2003) Mutations in the DJ-1 gene associated with autosomal recessive early-onset parkinsonism. Science 299:256–259

Brodersen DE, Nissen P (2005) The social life of ribosomal proteins. FEBS J 272:2098–2108

Calderan-Rodrigues MJ, Jamet E, Bonassi MB, Guidetti-Gonzalez S, Begossi AC, Setem LV, Franceschini LM, Fonseca JG, Labate

CA (2014) Cell wall proteomics of sugarcane cell suspension cultures. Proteomics 14:738–749
Carta S, Castellani P, Delfino L, Tassi S, Venè R, Rubartelli A (2009) DAMPs and inflammatory processes: the role of redox in the different outcomes. JLeukoc Biol 86:549–555
Chakrabarty J, Naik A, Fessler M, Munske G, Chowdhury S (2016) Differential tandem mass spectrometry-based cross-linker: a new approach for high confidence in identifying protein cross-linking. Anal Chem 18:10215–10222
Chan J, Crowell E, Eder M, Calder G, Bunnewell S, Findlay K, Vernhettes S, Höfte H, Lloyd C (2010) The rotation of cellulose synthase trajectories is microtubule dependent and influences the texture of epidermal cell walls in *Arabidopsis* hypocotyls. J Cell Sci 123:3490–3495
Chana-Muñoz A, Jendroszek A, Sønnichsen M, Wang T, Ploug M, Jensen JK, Andreasen PA, Bendixen C, Panitz F (2019) Origin and diversification of the plasminogen activation system among chordates. BMC Evol Biol 19:27
Chang SS, Prezelin BB, Trench RK (1983) Mechanisms of photoadaptation in three strains of the symbiotic dinoflagellate *Symbiodinium microadriaticum*. Mar Biol 76:219–229
Chao Y, Fan C, Liang Y, Gao B, Zhang S (2012) A novel serpin with antithrombin-like activity in *Branchiostoma japonicum*: implications for the presence of a primitive coagulation system. PLoS ONE 7(3):e32392. https://doi.org/10.1371/journal.pone.0032392
Chivasa S, Murphy AM, Hamilton JM, Lindsey K, Carr JP, Slabas AR (2009) Extracellular ATP is a regulator of pathogen defence in plants. Plant J 60:436–448
Clarke KR (1993) Non-parametric multivariate analyses of changes in community structure. Aust Ecol 18:117–143
Cohen J (1992a) A power primer. Psychol Bull 112:155–159
Cohen J (1992b) Statistical power analysis. Curr Dir Psychol Sci 1:98–101
Colombo-Pallotta MF, Rodriguez-Roman A, Iglesias-Prieto R (2010) Calcification in bleached and unbleached Montastraea faveolata: evaluating the role of oxygen and glycerol. Coral Reefs 29:899–907
Cvitanovic C, Wilson SK, Fulton CJ, Almany GR, Anderson P, Babcock RC, Ban NC, Beeden RJ, Beger M, Cinner J, Dobbs K, Evans LS, Farnham A, Friedman KJ, Gale K, Gladstone W, Grafton Q, Graham NAJ, Gudge S, Harrison PL, Holmes TH, Johnstone N, Jones GP, Jordan A, Kendrick AJ, Klein CJ, Little LR, Malcolm HA, Morris D, Possingham HP, Prescott J, Pressey RL, Skilleter GA, Simpson C, Waples K, Wilson D, Williamson DH (2013) Critical research needs for managing coral reef marine protected areas: perspectives of academics and managers. J Environ Manag 114:84–91
Davy SK, Allemand D, Weis VM (2012) Cell biology of cnidarian-dinoflagellate symbiosis. Microbiol Mol Biol Rev 76:229–261
Deniaud-Bouët E, Hardouina K, Potina P, Kloarega B, Hervé C (2017) A review about brown algal cell walls and fucose-containing sulfated polysaccharides: cell wall context, biomedical properties and key research challenges. Carbohydr Polym 175:395–408
Ebnet K (2017) Junctional adhesion molecules (JAMs): cell adhesion receptors with pleiotropic functions in cell physiology and development. Physiol Rev 97:1529–1554
Edmunds PJ, Spencer Davies P (1986) An energy budget for Porites porites (Scleractinia). Mar Biol 92:339–347
Elschenbroich S, Kim Y, Medin JA, Kislinger T (2010) Isolation of cell surface proteins for mass spectrometry-based proteomics. Expert Rev Proteom 7:141–154
Federica T, Antonio G (2018) Systematic review of plasma-membrane ecto-ATP synthase: a new player in health and disease. Exp Mol Pathol 104:59–70
Ferro M, Seigneurin-Berny D, Rolland N, Chapel A, Salvi D, Garin J, Joyard J (2000) Organic solvent extraction as a versatile procedure to identify hydrophobic chloroplast membrane proteins. Electrophoresis 21:3517–3526
Friedrich S, Konietschke F, Pauly M (2018) MANOVA.RM: analysis of multivariate data and repeated measures designs. R package version 0.3.2. https://github.com/smn74/MANOVA.RM
Furla P, Allemand D, Orsenigo MN (2000) Involvement of H(+)-ATPase and carbonic anhydrase in inorganic carbon uptake for endosymbiont photosynthesis. Am J Physiol Regul Integr Comp Physiol 278:R870–R881
Gancedo C, Flores CL, Gancedo JM (2016) The expanding landscape of moonlighting proteins in yeasts. Microbiol Mol Biol Rev 80:765–777
Gates RD, Baghdasarian G, Muscatine L (1992) Temperature stress causes host cell detachment in symbiotic cnidarians: implications for. Biol Bull 182:324–332
Greenland S, Stephen J, Senn SJ, Rothman KJ, Carlin JB, Poole C, Goodman SN, Altman DG (2016) Statistical tests, *P* values, confidence intervals, and power: a guide to misinterpretations. Eur J Epidemiol 31:337–350
Hahn M, Mendgen K (2001) Signal and nutrient exchange at biotrophic plant-fungus interfaces. Curr Opin Plant Biol 4:322–327
Hasanuzzaman M, Nahar K, Alam MM, Roychowdhury R, Fujita M (2013) Physiological, biochemical, and molecular mechanisms of heat stress tolerance in plants. Int J Mol Sci 14:9643–9684
Hassan S, Mathesius U (2012) The role of flavonoids in root-rhizosphere signalling: opportunities and challenges for improving plant–microbe interactions. J Exp Bot 63:3429–3444
Hoegh-Guldberg (1999) Climate change, coral bleaching and the future of the worldís coral reefs. Mar Freshw Res 50:839–866
Hoegh-Guldberg O, Mumby PJ, Hooten AJ, Steneck RS, Greenfield P, Gomez E, Harvell CD, Sale PF, Edwards AJ, Caldeira K, Knowlton N, Eakin CM, Iglesias-Prieto R, Muthiga N, Bradbury RH, Dubi A, Hatziolos ME (2007) Coral reefs under rapid climate change and ocean acidification. Science 318:1737–1742
Howes MT, Kirkham M, Riches J, Cortese K, Walser PJ, Simpson F, Hill MM, Jones A, Lundmark R, Lindsay MR, Hernandez-Deviez DJ, Hadzic G, McCluskey A, Bashir R, Liu L, Pilch P, McMahon H, Robinson PJ, Hancock JF, Mayor S, Parton RG (2010) Clathrin-independent carriers form a high capacity endocytic sorting system at the leading edge of migrating cells. J Cell Biol 190:675–691
Jeffery CJ (2015) Why study moonlighting proteins? Front genet 6:211. https://doi.org/10.3389/fgene.2015.00211
Jimbo M, Yamashita H, Koike K, Sakai R, Kamiya H (2010) Effects of lectin in the scleractinian coral *Ctenactis echinata* on symbiotic zooxanthellae. Fish Sci 76:355–363
Jo E, Webb S, Klemke G (2010) Cell signaling by urokinase-type plasminogen activator receptor induces stem cell–like properties in breast cancer cells. Cancer Res 70:8948–8958
Jones AR IV, Meshulam T, Oliveira MF, Burritt N, Corkey BE (2015) Extracellular redox regulation of intracellular reactive oxygen generation, mitochondrial function and lipid turnover in cultured human adipocytes. PLoS ONE 11(10):e0164011. https://doi.org/10.1371/journal.pone.0164011
Kamal AHM, Chakrabarty JK, Udden SMN, Zaki MdH, Chowdhury SM (2018) Inflammatory proteomic network analysis of statin-treated and lipopolysaccharide-activated macrophages. Sci Rep 8:164. https://doi.org/10.1038/s41598-017-18533-1
Karim W, Kaswadji R, Prartono T, Gorettipanggabean LM (2011) Growth and extracellular carbonic anhydrase activity of zooxanthellae *Symbiodinium* sp. in response of zinc enrichment. Hayati J Biosci 18:157–163
Koike K, Jimbo M, Sakai R, Kaeriyama M, Muramoto K, Ogata T, Maruyama T, Kamiya H (2004) Octocoral chemical signaling selects and controls dinoflagellate symbionts. Biol Bull 207:80–86

LaJeunesse TC, Parkinson JE, Gabrielson PW, Jeong HJ, Reimer JD, Voolstra CR, Santos SR (2018) Systematic revision of symbiodiniaceae highlights the antiquity and diversity of coral endosymbionts. Curr Biol 28:2570–2580

Lee SK, Kim Y, Kim SS, Lee JH, Cho K, Lee SS, Lee ZW, Kwon KH, Kim YH, Suh-Kim H, Yoo JS, Park YM (2009) Differential expression of cell surface proteins in human bone marrow mesenchymal stem cells cultured with or without basic fibroblast growth factor containing medium. Proteomics 9:4389–4405

Lee SY, Jeong HJ, Kang MS, Jang TY, Jang SH, Lim AS (2014) Morphological characterization of *Symbiodinium minutum* and *S. psygmophilum* belonging to clade B. Algae 29:299–310

Lemmon MA, Freed DM, Schlessinger J, Kiyatkin A (2016) The dark side of cell signaling: positive roles for negative regulators. Cell 164:1172–1184

Li C, Wang DaZhi, Dong H, Xie Z, Hong H (2012) Proteomics of a toxic dinoflagellate *Alexandrium catenella* DH01: detection and identification of cell surface proteins using fluroescent labeling. Sci Bull 57:3320–3327

Li H, Huang Z, Ye S, Lu C, Cheng P, Chen S, Chen C (2013) Membrane labeling of coral gastrodermal cells by biotinylation: the proteomic identification of surface proteins involving cnidaria-dinoflagellate endosymbiosis. PLoS ONE 9(1):e85119. https://doi.org/10.1371/journal.pone.0085119

Liew YJ, Aranda M, Voolstra CR (2016) Reefgenomics.Org—a repository for marine genomics data. Database. https://doi.org/10.1093/database/baw152

Lin S, Cheng S, Song B, Zhong X, Lin X, Li W, Li L, Zhang Y, Zhang H, Ji Z, Cai M, Zhuang Y, Shi X, Lin L, Wang L, Wang Z, Liu X, Yu S, Zeng P, Hao H, Zou Q, Chen C, Li Y, Wang Y, Xu C, Meng S, Xu X, Wang J, Yang H, Campbell DA, Sturm NR, Dagenais-Bellefeuille S, Morse D (2015) The Symbiodinium kawagutii genome illuminates dinoflagellate gene expression and coral symbiosis. Science 350:691–694

Little AF, van Oppen MJ, Willis BL (2004) Flexibility in algal endosymbioses shapes growth in reef corals. Science 304:1492–1494

Logan D, LaFlamme A, Weis V, Davy S (2010) Flow-cytometric characterization of the cell-surface glycans of symbiotic dinoflagellates (*Symbiodinium* Spp.). J Phycol 46:525–533

Madeira F, Park YM, Lee J, Buso N, Gur T, Madhusoodanan N, Basutkar P, Tivey ARN, Potter SC, Finn RD, Lopez R (2019) The EMBL-EBI search and sequence analysis tools APIs in 2019. Nucleic Acids Res. https://doi.org/10.1093/nar/gkz268

Madsen EB, Antolín-Llovera M, Grossmann C, Ye J, Vieweg S, Broghammer A, Krusell L, Radutoiu S, Jensen ON, Stougaard J, Parniske M (2011) Autophosphorylation is essential for the in vivo function of the Lotus japonicus Nod factor receptor 1 and receptor-mediated signalling in cooperation with Nod factor receptor 5. Plant J 65:404–417

Majetschak M (2011) Extracellular ubiquitin: immune modulator and endogenous opponent of damage-associated molecular pattern molecules. J Leukoc Biol 89:205–219

Mayfield AB, Chen Y-J, Lu C-Y, Chen C-S (2018) The proteomic response of the reef coral *Pocillopora acuta* to experimentally elevated temperatures. PLoS ONE 13(1):e0192001. https://doi.org/10.1371/journal.pone.0192001

McGinty E, Pieczonka J, Mydlarz L (2012) Variations in reactive oxygen release and antioxidant activity in multiple symbiodinium types in response to elevated temperature. Microb Ecol 64:1000–1007

Merselis DG, Lirman D, Rodriguez-Lanetty M (2018) Symbiotic immuno-suppression: is disease susceptibility the price of bleaching resistance? PeerJ 6:e4494. https://doi.org/10.7717/peerj.4494

Miles M, Voolstra CR, Castro CB, Pires DO, Calderon EN, Sumida PYG (2017) Expression of a symbiosis-specific gene in *Symbiodinium* type A1 associated with coral, nudibranch and giant clam larvae. R Soc Open Sci 4:170253. https://doi.org/10.1098/rsos.170253

Mohamed AR, Cumbo V, Harii S, Shinzato C, Chan CX, Ragan MA, Bourne DG, Willis BL, Ball EE, Satoh N, Miller DJ (2016) The transcriptomic response of the coral *Acropora digitifera* to a competent *Symbiodinium* strain: the symbiosome as an arrested early phagosome. Mol Ecol 25:3127–3141

Mustaffa NIH, Striebel M, Wurl O (2017) Enrichment of extracellular carbonic anhydrase in the sea surface microlayer and its effect on air–sea CO_2 exchange. Geophys Res Lett 44:324–330

Oakley CA, Davy SK (2018) Cell biology of coral bleaching. In: van Oppen MJH, Lough JM (eds) Coral bleaching: patterns, processes, causes and consequences. Springer International Publishing, Switzerland, pp 189–211

Ochs J, LaRue T, Tinaz B, Yongue C, Domozych DS (2014) The cortical cytoskeletal network and cell-wall dynamics in the unicellular charophycean green alga Penium margaritaceum. Ann Bot 114:1237–1249

Oksanen J, Blanchet FG, Friendly M, Kindt R, Legendre P, McGlinn D, Minchin PR, O'Hara RB, Simpson GL, Solymos P, Stevens MHH, Szoecs E, Wagner H (2018) vegan: Community Ecology Package. R package version 2.5–3. https://CRAN.R-project.org/package=vegan

Oldroyd GE, Downie JA (2004) Calcium, kinases and nodulation signalling in legumes. Nat Rev Mol Cell Biol 5:566–576

Orjalo AV, Bhaumik D, Gengler BK, Scott GK, Campisi J (2009) Cell surface-bound IL-1alpha is an upstream regulator of the senescence-associated IL-6/IL-8 cytokine network. Proc Natl Acad Sci USA 106:17031–17036

Park SY, Kim IS (2017) Engulfment signals and the phagocytic machinery for apoptotic cell clearance. Exp Mol Med 49:e331

Parkinson JE, Baumgarten S, Michell CT, Baums IB, LaJeunesse TC, Voolstra CR (2016) Gene Expression variation resolves species and individual strains among coral-associated dinoflagellates within the genus *Symbiodinium*. Genome Biol Evol 8:665–680

Parkinson JE, Tivey TR, Mandelare PE, Adpressa DA, Loesgen S, Weis VM (2018) Subtle differences in symbiont cell surface glycan profiles do not explain species-specific colonization rates in a model cnidarian-algal symbiosis. Front Microbiol 9:842. https://doi.org/10.3389/fmicb.2018.00842

Pelz T, Drose DR, Fleck D, Henkel B, Ackels T, Spehr M, Neuhaus EM (2018) An ancestral TMEM16 homolog from *Dictyostelium discoideum* forms a scramblase. PLoS ONE 13(2):e0191219. https://doi.org/10.1371/journal.pone.0191219

R Development Core Team (2015) R: a language and environment for statistical computing. R Foundation for Statistical Computing, Vienna, Austria. https://www.R-project.org/

Rice ME, Harris GT (2005) Comparing effect sizes in follow-up studies: ROC area, Cohen's *d*, and *r*. Law Hum Behav 5:615–620

Robinson DG, Ding Y, Jiang L (2016) Unconventional protein secretion in plants: a critical assessment. Protoplasma 253:31–43

Roche P, Maillet F, Plazanet C, Debellé F, Ferro M, Truchet G, Promé JC, Dénarié J (1996) The common nodABC genes of *Rhizobium meliloti* are host-range determinants. Proc Natl Acad Sci 93:15305–15310

Rodrigues ML, Godinho RM, Zamith-Miranda D, Nimrichter L (2015) Traveling into outer space: unanswered questions about fungal extracellular vesicles. PLoS Pathog 11:e1005240

Samuel M, Bleackley M, Anderson M, Mathivanan S (2015) Extracellular vesicles including exosomes in cross kingdom regulation: a view-point from plant–fungal interactions. Front Plant Sci 6:766

Sarras M, Deutzmann R (2001) Hydra and Niccolo Paganini (1782–1840)—two peas in a pod? The molecular basis of extracellular matrix structure in the invertebrate, *Hydra*. BioEssays 23:716–724

Scotcher D, Billington S, Brown J, Jones CR, Brown CDA, Rostami-Hodjegan A, Galetin A (2017) Microsomal and cytosolic scaling factors in dog and human kidney cortex and application for in vitro-in vivo extrapolation of renal metabolic clearance. Drug Metab Dispos 45:556–568

Shi L, Dong H, Reguera G, Beyenal H, Lu A, Liu J, Yu HQ, Fredrickson JK (2016) Extracellular electron transfer mechanisms between microorganisms and minerals. Nat Rev Microbiol 1:651–662

Shimus, Levy, Herman (1985) A chemically cleavable biotinylated nucleotide: usefulness in the recovery of protein-DNA complexes from avidin affinity columns. Proc Natl Acad Sci 82:2593–2597

Shomer, Novacky, Pike, Yermiyahu, Kinraide (2003) Electrical potentials of plant cell walls in response to the ionic environment. Plant Physiol 133:411–422

Slabas AR, Ndimba B, Simon WJ, Chivasa S (2004) Proteomic analysis of the *Arabidopsis* cell wall reveals unexpected proteins with new cellular locations. Biochem Soc Trans 32:524–528

Smith S, Boitz J, Chidambaram ES, Chatterjee A, AitTihyaty M, Ullman B, Jardim A (2016) The cystathionine-β-synthase domains on the guanosine 5″-monophosphate reductase and inosine 5′-monophosphate dehydrogenase enzymes from Leishmania regulate enzymatic activity in response to guanylate and adenylate nucleotide levels. Mol Microbiol 100:824–840

Sogin EM, Putnam HM, Nelson CE, Anderson P, Gates RD (2017) Correspondence of coral holobiont metabolome with symbiotic bacteria, archaeaand Symbiodinium communities. Environ Microbiol Rep 9:310–315

Spalding M, Burke L, Wood SA, Ashpole J, Hutchison J, Ermgassen P (2017) Mapping the global value and distribution of coral reef tourism. Mar Policy 82:104–113

Suzuki M, Van Paesschen W, Stalmans I, Horita S, Yamada H, Bergmans BA, Legius E, Riant F, De Jonghe P, Lia Y, Sekine T, Igarashi T, Fujimoto I, Mikoshiba K, Shimadzu M, Shiohara M, Braverman N, Al-Gazali L, Fujita T, Seki G (2010) Defective membrane expression of the Na+–HCO_3_ cotransporter NBCe1 is associated with familial migraine. Proc Natl Acad Sci 107:15963–15968

Torchiano M (2018) Efficient effect size computation. R package version 0.7.4. https://github.com/mtorchiano/effsize/

Ünal CM, Steinert M (2014) Microbial peptidyl-prolyl cis/trans isomerases (PPIases): virulence factors and potential alternative drug targets. Microbiol Mol Biol Rev 78:544–571

Vu V (2011) A ggplot2 based biplot. R package version 0.55. https://github.com/vqv/ggbiplot

Wang W, Jeffery CJ (2016) An analysis of surface proteomics results reveals novel candidates for intracellular/surface moonlighting proteins in bacteria. Mol Biosyst 12:1420–1431

Wang SB, Hu Q, Sommerfeld M, Chen F (2004a) Cell wall proteomics of the green alga *Haematococcus pluvialis* (Chlorophyceae). Proteomics 4:692–708

Wang W, Vinocur B, Shoseyov O, Altman A (2004b) Role of plant heat-shock proteins and molecular chaperones in the abiotic stress response. Trends Plant Sci 9:244–252

Wang R, Town T, Gokarn V, Flavell RA, Chandawarkar RY (2006) HSP70 enhances macrophage phagocytosis by interaction with lipid raft-associated TLR-7 and upregulating p38 MAPK and PI3K pathways. J Surg Res 36:58–69

Wang DZ, Dong HP, Li C, Xie ZX, Lin L, Hong HS (2011) Identification and characterization of cell wall proteins of a toxic dinoflagellate *Alexandrium catenella* using 2-D DIGE and MALDI TOF-TOF mass spectrometry. Evid Based Complement Alternat Med 2011:984080. https://doi.org/10.1155/2011/984080

Wang Q, Liu J, Zhu H (2018) Genetic and molecular mechanisms underlying symbiotic specificity in legume–rhizobium interactions. Front Plant Sci 9:313

Warton DI, Wright ST, Wang Y (2012) Distance-based multivariate analyses confound location and dispersion effects. Methods Ecol Evol 3:89–101

Wasserstein RL, Lazar NA (2016) ASA statement on statistical significance and *P* values. Am Stat 70:129–133

Weis V (2008) Cellular mechanisms of Cnidarian bleaching: stress causes the collapse of symbiosis. J Exp Biol 211:3059–3066

Weston AJ, Dunlap WC, Shick JM, Klueter A, Iglic K, Vukelic A, Starcevic A, Ward M, Wells ML, Trick CG, Long PF (2012) A profile of an endosymbiont-enriched fraction of the coral *Stylophora pistillata* reveals proteins relevant to microbial-host interactions. Mol Cell Proteomics 11(M111):015487. https://doi.org/10.1074/mcp.M111.015487

Wiersma VR, Michalak M, Abdullah TM, Bremer E, Eggleton P (2015) Mechanisms of translocation of ER chaperones to the cell surface and immunomodulatory roles in cancer and autoimmunity. Front Oncol 5:7. https://doi.org/10.3389/fonc.2015.00007

Wilhelm M, Schlegl J, Hahne JH, Gholami AM, Lieberenz M, Savitski MM, Ziegler E, Butzmann L, Gessulat S, Marx H, Mathieson T, Lemeer S, Schnatbaum K, Reimer U, Wenschuh H, Mollenhauer M, Slotta-Huspenina J, Boese JH, Bantscheff M, Gerstmair A, Faerber F, Kuster B (2014) Mass-spectrometry-based draft of the human proteome. Nature 509:582–587

Wood-Charlson E, Hollingworth L, Krupp D, Weis V (2006) Lectin/glycan interactions play a role in recognition in a coral/dinoflagellate symbiosis. Cell Microbiol 8:1985–1993

Wrobel L, Topf U, Bragoszewski P, Wiese S, Sztolsztener ME, Oeljeklaus S, Varabyova A, Lirski M, Chroscicki P, Mroczek S, Januszewicz E, Dziembowski A, Koblowska M, Warscheid B, Chacinska A (2015) Mistargeted mitochondrial proteins activate a proteostatic response in the cytosol. Nature 524:485–488

Yang SH, Liu R, Perez EJ, Wen Y, Stevens SM Jr, Valencia T, Brun-Zinkernagel AM, Prokai L, Will Y, Dykens J, Koulen P, Simpkins JW (2004) Mitochondrial localization of estrogen receptor beta. Proc Natl Acad Sci 101:4130–4135

Yellowlees D, Dionisio-Sese ML, Masuda K, Maruyama T, Abe T, Baillie B, Tsuzuki M, Miyachi S (1993) Role of carbonic anhydrase in the supply of inorganic carbon to the giant clam—zooxanthellate symbiosis. Mar Biol 115:605–611